Event detection in P-SV prestack time migration using matched filters

Jeff K. Beckett and John C. Bancroft

ABSTRACT

Given a particular statistical measure of signal to noise (S/N), the "matched filter" is the ideal linear filter for maximizing the S/N ratio of a signal amongst random noise (Robinson & Treitel, 1980). Kirchhoff migration is a seismic processing equivalent to the matched filter. Through improved approximations of the earth's impulse response, superior output S/N ratios, or superior imaging, can be obtained. In this paper, a matched filter approach to prestack P-SV wave amplitude weighting is proposed, and preliminary tests on synthetic data yield promising results.

INTRODUCTION

The chief purpose of migration is to reconstruct an image of the subsurface from seismic reflection data. Conventional P-SV wave Kirchhoff prestack migration involves the summation over scatterpoint traveltime impulse responses where a T_0/T scaling factor is applied to each input sample. P-SV wave reflection coefficients generally approach zero as the source-receiver offset approaches zero, in constant velocity, isotropic media. Therefore, application of the T_0/T scaling factor alone poorly approximates the earth's impulse response. A new weighting function is thus proposed to improve upon the output S/N ratio of P-SV migration through improved estimates of the impulse response.

First, an introduction to matched filter theory will be given, followed by a discussion of the relationship between the theory and Kirchhoff migration. An overview of P-SV wave kinematics will follow to facilitate the understanding of the method of migration used in the synthetic example.

THEORY

The Matched Filter

Assuming a known input signal in random, white noise, the matched filter is designed to maximize the signal to noise (S/N) ratio, μ. Defined as the ratio of the square of signal amplitude to the square of noise amplitude, μ is given by (Lathi, 1965)

$$\mu = s_0^{\,2}(t_m) \Big/ \overline{n_0^{\,2}(t_m)}, \tag{1}$$

where $s_0(t_m)$ is the output signal and $n_0(t_m)$ is the output noise at time t_m. The mean value of the noise is used, as the noise is random. A diagram of the matched filter is shown in Figure 1. ,

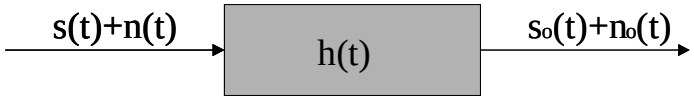

FIG. 1. The matched filter.

where $h(t)$ is the function of the desired optimum filter. It may be shown that μ can be maximized through selecting a filter, $h(t)$, such that (Lathi, 1965):

$$h(t) = F^{-1}\left(kS(-\omega)e^{-j\omega t_m}\right), \tag{2}$$

Where $S(-\omega)$ is the Fourier transform of the time reversed input signal, $e^{-j\omega t_m}$ represents a time shift of t_m time units, and k is an arbitrary constant. Through crosscorrelation of the input signal with the known impulse response, the ideal output S/N ratio is achieved.

Kirchhoff migration is a seismic processing equivalent to matched filtering. It is assumed that the poststack seismic model is the convolution of scatterpoint reflection coefficients with diffractions, amongst random noise. The input is the stacked section, and the earth's impulse response is the diffraction. Crosscorrelation of the diffraction with the data yields the output migrated image. The S/N ratio (event detection) of the migration is maximized when the impulse response is known. Therefore, through better estimates of the earth's impulse response, superior imaging can be achieved. The same argument holds for prestack migration, where the input is now a 3D prestack volume, and the scatterpoint traveltime impulse response is a surface defined by the double square root (DSR) equation (Bancroft, 2000).

CONVERTED WAVE KINEMATICS

Consider the prestack geometry in Figure 2, where *h* is half of the source-receiver offset, z_0 is the depth of the scatterpoint, and *x* is the source-receiver midpoint relative to the scatterpoint.

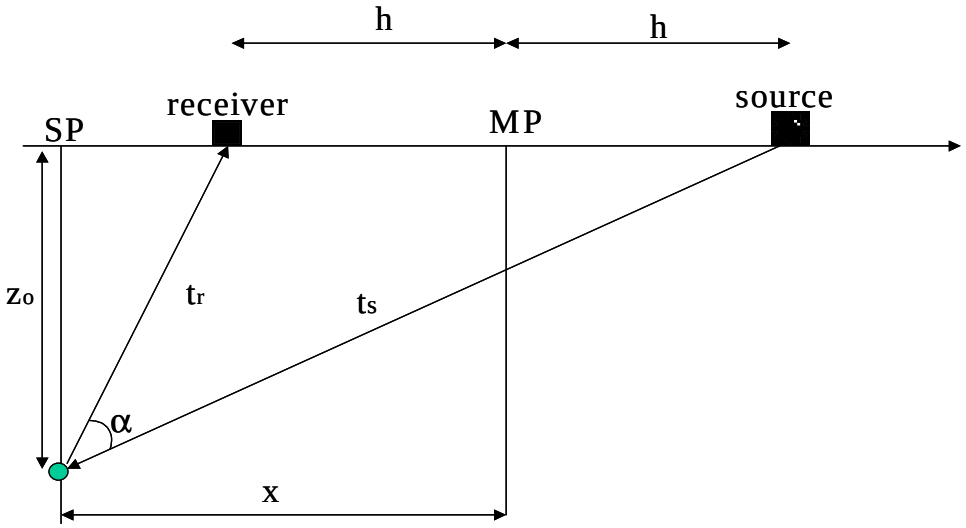

FIG. 2. Prestack time migration geometry showing traveltime from source to scatterpoint, t_s, and traveltime from scatterpoint to receiver, t_r.

The total traveltime from source to receiver in isotropic, constant velocity media is given by (Bancroft et al.,1998).

$$t = t_s + t_r, \tag{3}$$

The P-P wave energy traveltime surface for a scatterpoint in constant velocity is known as "Cheops pyramid", and is defined by the DSR equation (Bancroft et al., 1998)

$$t = \left(\frac{z_0^2 + (x+h)^2}{V_p{}^2} \right)^{1/2} + \left(\frac{z_0^2 + (x-h)^2}{V_p{}^2} \right)^{1/2}, \tag{4}$$

where V_P is the P-wave velocity, and is constant. An example of Cheops pyramid is shown in Figure 3. Prestack migration is accomplished through crosscorrelation of the traveltime surface with the prestack data.

Consider now the prestack volume of a scatterpoint using converted waves. The traveltime surface is again given by the DSR equation, however it is a modified version of equation (4) as it incorporates shear wave velocity from the scatterpoint to the receiver. The converted wave DSR equation is now given by;

$$t = \left(\frac{z_0^2 + (x+h)^2}{V_P{}^2} \right)^{1/2} + \left(\frac{z_0^2 + (x-h)^2}{V_S{}^2} \right)^{1/2}, \tag{5}$$

where Vs is the shear wave velocity. By letting V_P = 800m/s, V_S= 400m/s, and holding the other parameters the same as in Figure 3, the traveltime surface can be calculated and is shown in Figure 4.

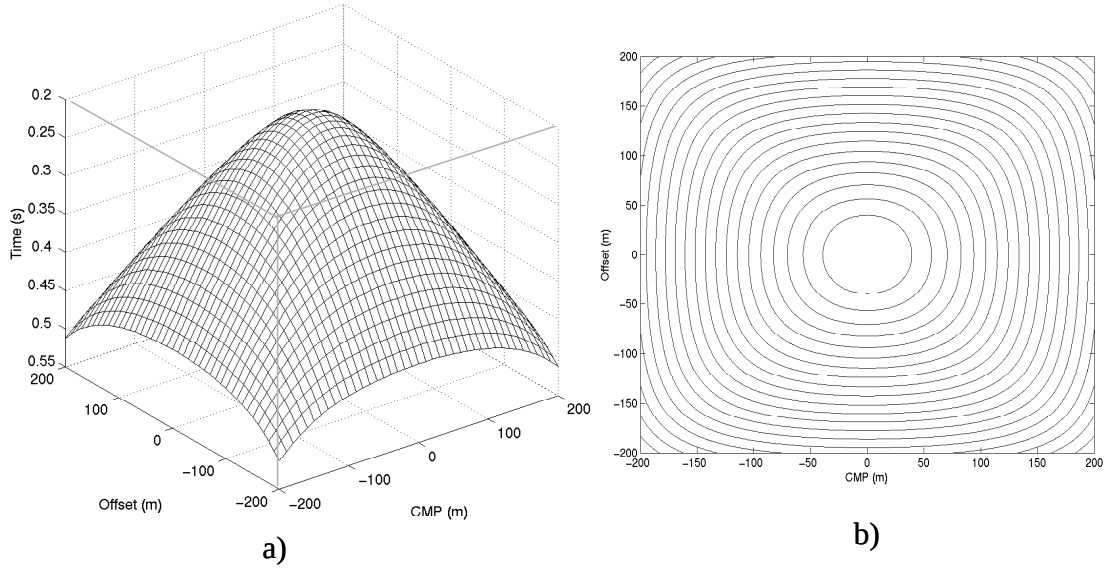

FIG. 3. a) Perspective view of a P-P wave traveltime surface for a scatterpoint located at $z_0 = 100m$. $V_P = 800m/s$. b) Plan view of (a) showing contour lines of constant traveltimes

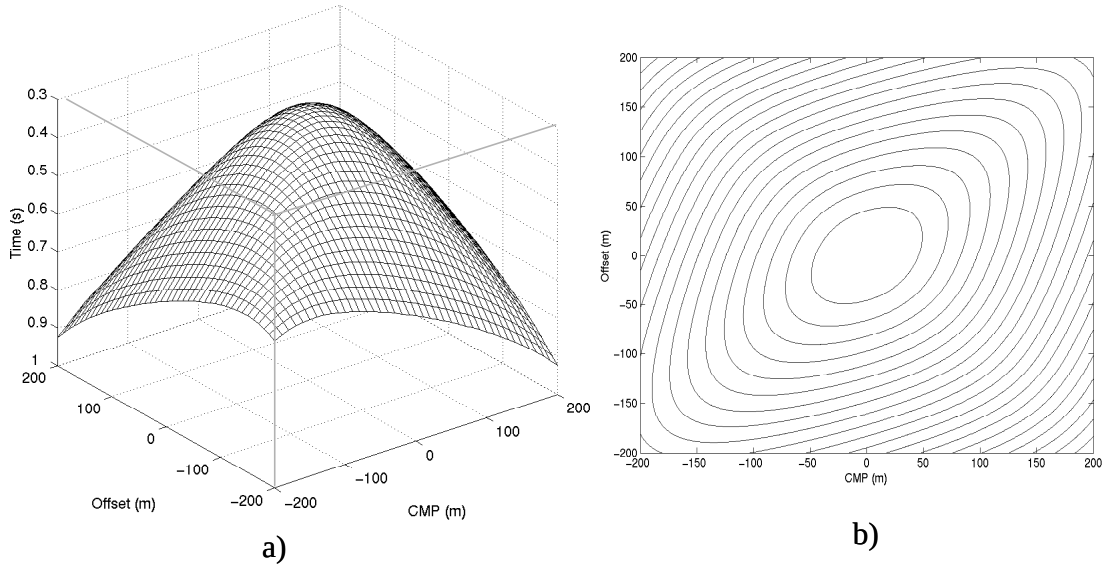

FIG. 4 a) Perspective view of a P-SV wave traveltime surface for a scatterpoint located at z_0=100m. V_P=800m/s, and V_S=400m/s. b) Plan view of (a) showing contour lines of constant traveltimes.

Observe that the converted wave traveltime surface (Figure 4) differs from the P-P case (Figure 3) in that it appears to be biased along the line $x = h$. This shape change is due to the asymmetry of P-SV wave raypaths. Conventional Kirchhoff prestack migration of P-SV data entails summing over each traveltime surface, and placing the energy at the scatterpoint location. Corrections are made to compensate for spherical divergence, obliquity (T_0/T), and wavelet distortion (Bancroft, 2000).

MIGRATION

According to matched filter theory, improved impulse response estimation results in improved output S/N ratio. The proposed migration method suggests approximating the impulse response by weighting each sample on a traveltime surface by the appropriate Zoeppritz defined reflection coefficient at the scatterpoint.

Consider the P-SV traveltime surface shown in Figure 4. Given the geometry in Figure 2, the angles of incidence all *x* and *h* locations may be calculated. It is assumed that the scatterpoint is a reflective element with a particular dip angle. The angle between the down going and up going rays, α, is given by:

$$\alpha = \tan^{-1}\left(\frac{x+h}{z_0}\right) - \tan^{-1}\left(\frac{x-h}{z_0}\right), \tag{6}$$

and,

$$\alpha = \theta_i + \theta_r, \tag{7}$$

where θ_i is the angle of incidence and θ_r is the angle of reflection. Using Snell's Law we obtain:

$$\frac{V_p}{V_s} = \frac{\sin\theta_i}{\sin\theta_r} \tag{8}.$$

Assuming that $\frac{\sin\theta_i}{\sin\theta_r} \approx \frac{\theta_i}{\theta_r}$, and upon substitution of (8) into (7), θ_i is given as:

$$\theta_i = \frac{\alpha}{\left(1+\gamma^{-1}\right)}, \tag{9}$$

where γ is the V_P/V_S ratio.

Shown in Figure 5 is the % error in the approximation used in equation (8) where

$$\%Error = \left(\frac{\left(\frac{\sin\theta_i}{\sin\theta_r} - \frac{\theta_i}{\theta_r}\right)}{\left(\frac{\sin\theta_i}{\sin\theta_r}\right)}\right) * 100 \tag{10}$$

.

It is shown that for a V_P/V_S ratio of 2, the error in θ_i ranges from 0% (at θ_i~0°) to 5% (at θ_i~35°) to 10% (at θ_i ~45°). Errors in excess of ±10% are not presented in the figure. This source of error will be considered in the migration algorithm.

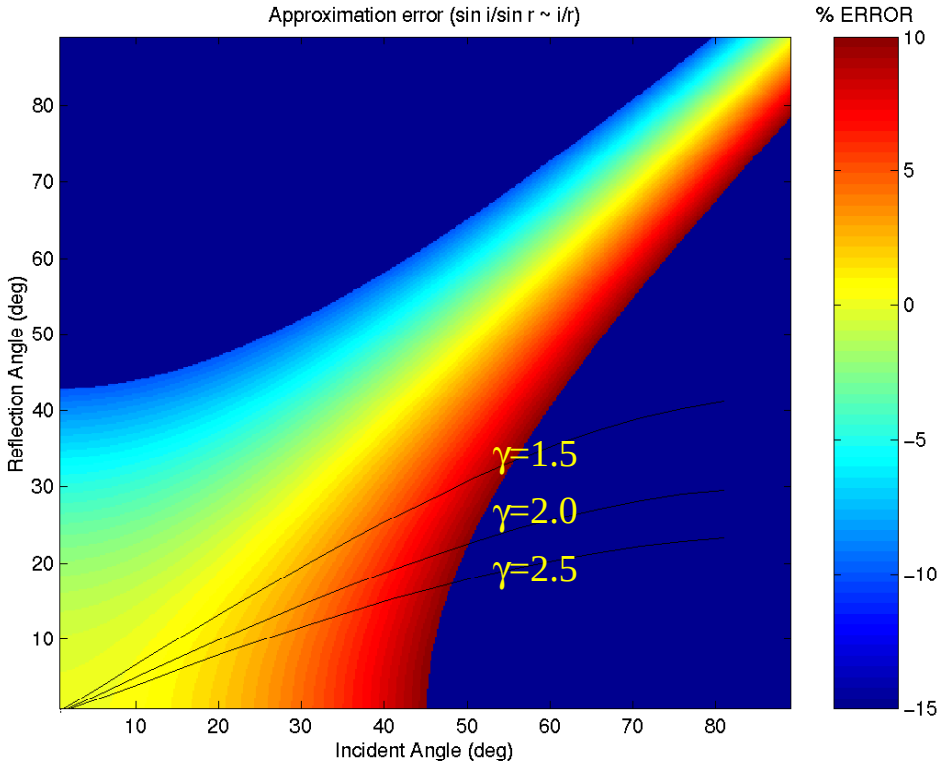

FIG. 5. Approximation error in assuming $\frac{\sin\theta_i}{\sin\theta_r} \approx \frac{\theta_i}{\theta_r}$.

Assuming that the scatterpoint is a dipping, elemental reflector, Zoeppritz defined reflection coefficients may be calculated for all source-receiver locations. Incident angles for all source-receiver pairs over a scatterpoint are calculated using equations (6) and (9). Contours of constant incident angles versus CMP and Offset are shown in Figure 6.

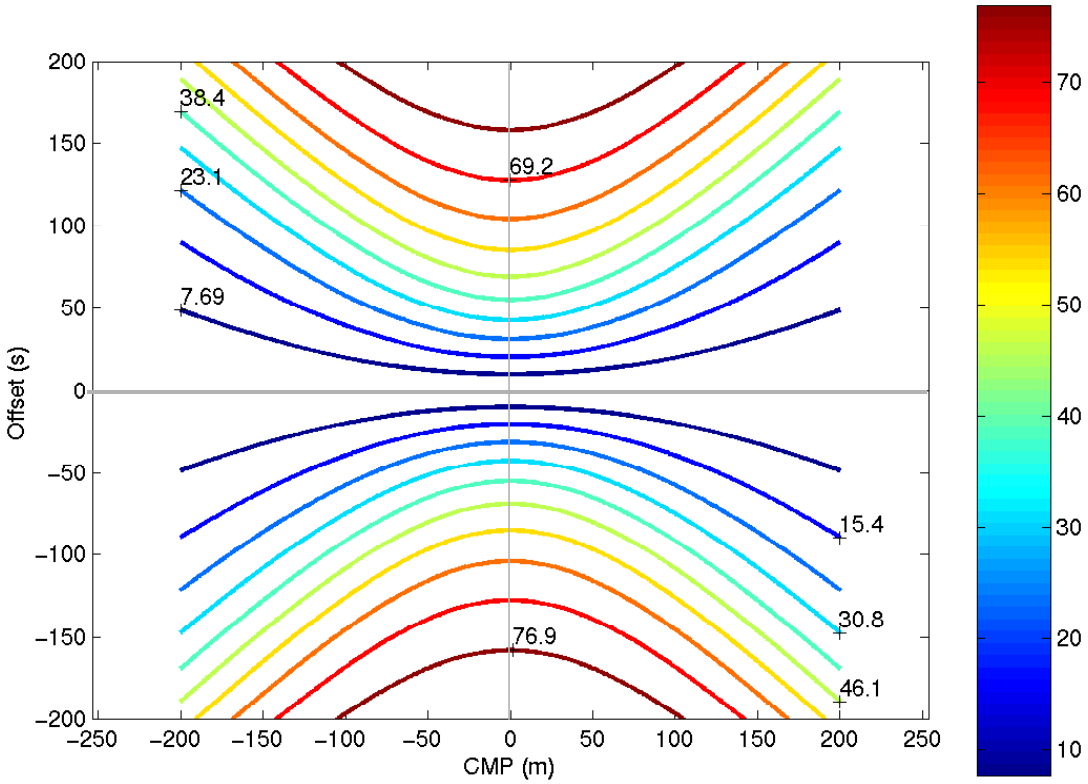

FIG. 6. Contour plot of angle of incidence versus CMP and offset. Angles are in degrees.

The reflection coefficient surface for all CMP-offset pairs may now be computed through solving the Zoeppritz equations given a set of velocity and density parameters shown in table 1.

Table.1.Velocity and density parameters for medium and scatterpoint

	Vp(m/s)	Vs(m/s)	ρ(kg/m^3)
Medium	2400	1200	4450
Scatterpoint	2100	1050	2100

These parameters were chosen to obtain a large range of reflection coefficients for the given range of incident angles, and were not chosen for any geological significance. The reflection coefficient surface is shown in Figure 7.

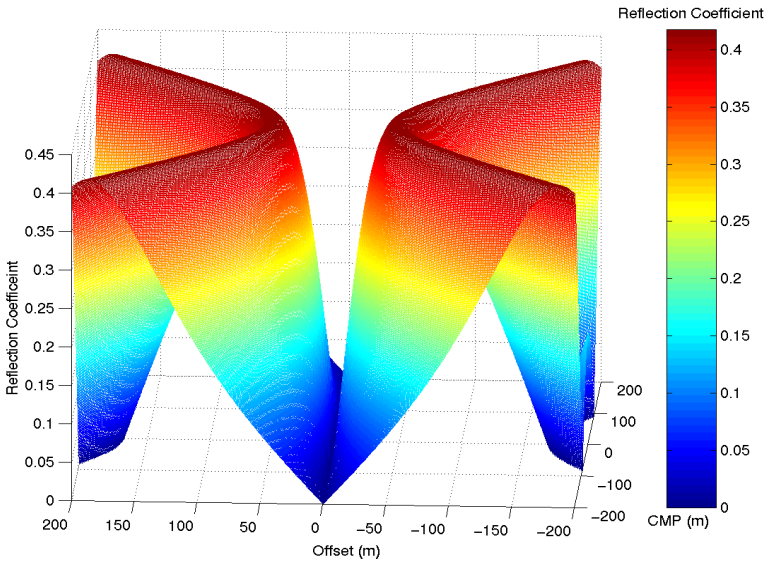

FIG. 7. P-S wave reflection amplitudes calculated from the Zoeppritz equations. Parameters used found in table 1.

The Kirchhoff migration is performed by first scaling each sample on the traveltime surface by the corresponding reflection coefficient as shown in Figure 8. Summation over the traveltime surface, and placing the energy back at the scatterpoint completes the migration. This process is repeated for every output sample.

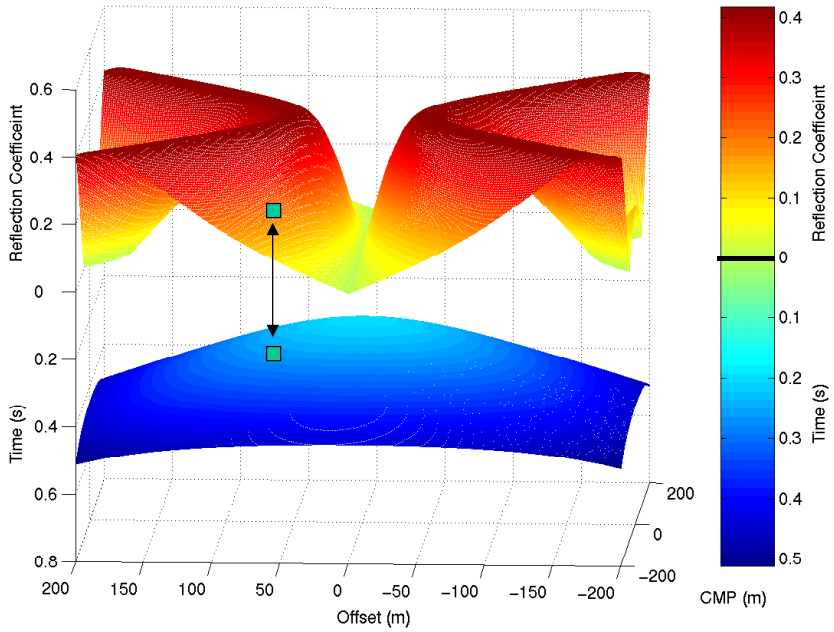

FIG. 8. Zoeppritz defined reflection coefficient surface plotted over a traveltime surface. Sample located at CMP(x),Offset(x) is shown to be scaled by reflection coefficient at CMP(x),Offset(x).

The Equivalent Offset Method (EOM) of prestack time migration is computationally fast and provides excellent velocity information. This technique is based on and includes all of the benefits of Kirchhoff time prestack migration, and may be applied to both P- wave and P-S data (Bancroft et al.,1998). EOM is thus chosen for the analysis.

EOM is founded on the principles of equivalent offsets and common conversion point (CCSP) gathers. The equivalent offset is used to enable the gathering of input samples prior to any time shifting. This transformation of P-SV data into CCSP gathers removes the asymmetry imposed by the P-SV raypaths. Equivalent offsets are chosen such that the total traveltime from source to receiver, t, is equal to that of a co-located source and receiver, $2t_e$. As shown in Figure 9, h_e is the equivalent offset from the CCSP surface location.

The key idea of EOM is the reformulation of equation (5) into one with a single square root. Assuming that the pseudo depth of a CCSP is z_0 and P-wave and S-wave velocities at this depth are $V_{P\ mig}$ and $V_{S\ mig}$ respectively, then $\gamma_{mig} = V_{P\,mig} / V_{S\,mig}$ expresses their migration velocity ratio. Equating (10) with the traveltimes for a co-located source and receiver yields (Wang et al.)

$$t = \left(\frac{Z_0^2 + (x+h)^2}{V_{P\,mig}^2} \right)^{1/2} + \left(\frac{Z_0^2 + (x-h)^2}{V_{S\,mig}^2} \right)^{1/2} = \left(\frac{Z_0^2 + h_e^{\,2}}{V_{P\,mig}^2} \right)^{1/2} + \left(\frac{Z_0^2 + h_e^{\,2}}{V_{S\,mig}^2} \right)^{1/2}, \quad 11)$$

(

It may be shown that (Wang et al.)

$$h_e = \left(\frac{T^2 V_{P\,mig}^2}{\left(1+\gamma_{mig}\right)^2} - Z_0^2 \right)^{1/2}, \quad (12)$$

where

$$Z_0^2 = \frac{C_2^2 - 2C_1 \pm C_2 \left(C_2^2 + 4h_s^2 - 4C_1 \right)^{1/2}}{2}, \quad (13)$$

$$C_1 = \frac{T^2 V_{P\,mig}^2 + h_s^2 - \gamma_{mig}^2 h_r^2}{1 - \gamma_{mig}^2}, \quad (14)$$

and

$$C_1 = \frac{2TV_{P\,mig}}{1 - \gamma_{mig}^2}. \quad (15)$$

The CCSP gathers are scaled, filtered to zero-phase, and corrected for normal moveout (NMO). Stacking of the CCSP gather produces the output migrated trace.

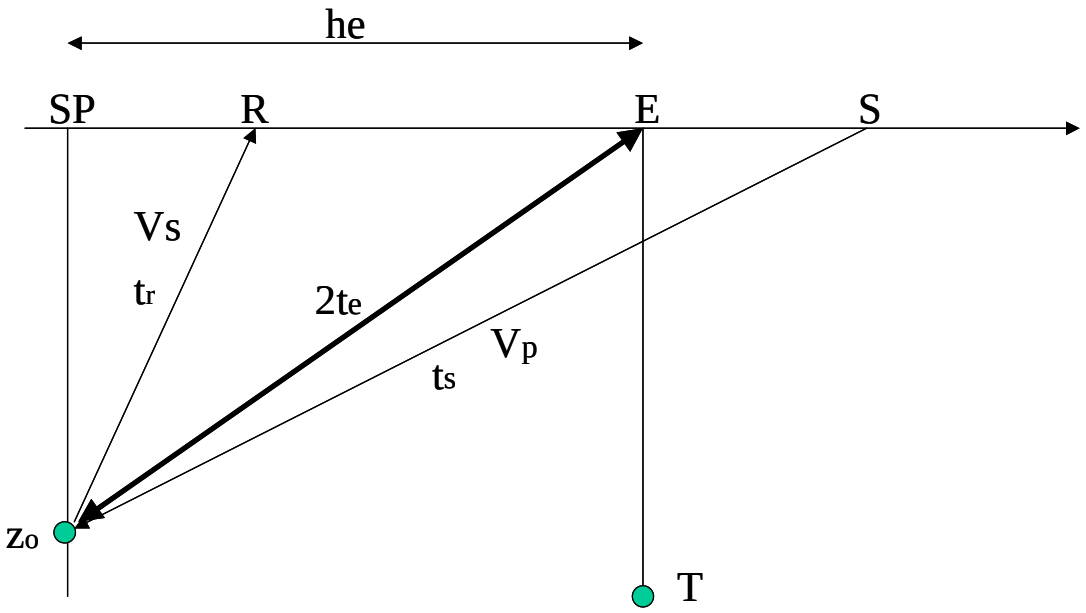

FIG.9. The position of the equivalent offset and traveltimes for a conversion scatterpoint

SYNTHETIC EXAMPLE

Synthetic P-SV prestack data were created for a flat reflector model using MATLAB. The acquisition parameters are given in table 2, and the elastic parameters are identical to those shown in table 1, where the properties of the 2nd layer are equivalent to those of the scatterpoint. The acoustic parameters were again chosen to incorporate a large range of reflection coefficients.

Table .2. Acquisition parameters used in split-spread experiment

sample int (ms)	shot int.(m)	rec.int.(m)	shot range(m)	max-min s-r offset (m)	depth to reflector (m)
2	25	25	0 to 2500	-1250 to 1250	400

An example of a shot recorded over a flat reflector with and without the addition of noise is shown in Figure 10 and Figure 11 respectively. A 30-Hz Ricker wavelet is used as the source. Noise was added to the section such that the signal to noise ratio equals 1. The RMS value of the signal on an arbitrary pilot trace is calculated and the standard deviation of the noise is given as: noise power = (signal power) / (signal to noise ratio). For each prestack trace, a pseudo random noise vector was calculated and added to the trace. A S/N ratio of 1 was used in calculating noise for all traces. Polarity has also been reversed for traces with negative offsets. Diffraction amplitudes were corrected for geometrical spreading and scaled by the appropriate Zoeppritz defined reflection coefficients

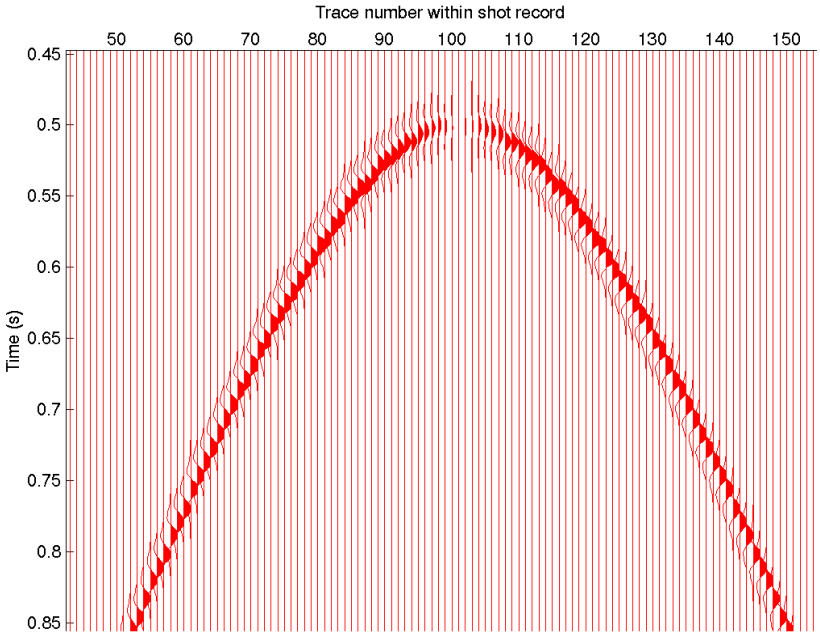

FIG.10. Shot record of a flat reflector model (zoomed in). No noise present.

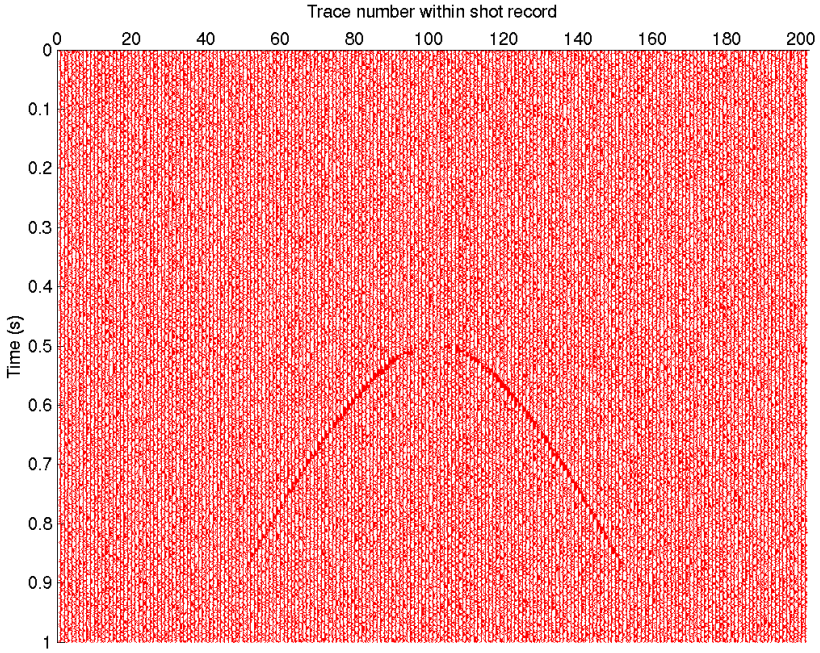

FIG.11. Shot record shown in Figure 10 with the addition of noise. S/N =1.

A CSP gather located at x=1250m without any additional amplitude scaling is shown in Figure 12. The same CSP gather with amplitudes scaled by the matched filter is shown in Figure 13. Both gathers are dip-limited to 45°. High amplitude noise is apparent along the dip limits of both figures as a dip limit taper is yet to be implemented in the CSP algorithm. The chief difference between the two figures is

that the amplitude filtered gather exhibits much less relative noise, particularly at shorter equivalent offsets. This effect is due to the scaling of samples by near zero reflection coefficient values.

A comparison of the final output migrations is shown in Figure 14. Ten *non*-match filtered CSP gathers, were corrected for NMO, filtered to zero-phase, stacked, and displayed as the first 10 traces in Figure 14 (from left to right). The same process was repeated for the ten match-filtered gathers, and the migrated traces constitute the remaining ten traces in Figure 14. All traces in the figure are plotted using the same scaling factor.

Notice that the match filter has succeeded in increasing the S/N ratio, and thus imaging, of the output migration.

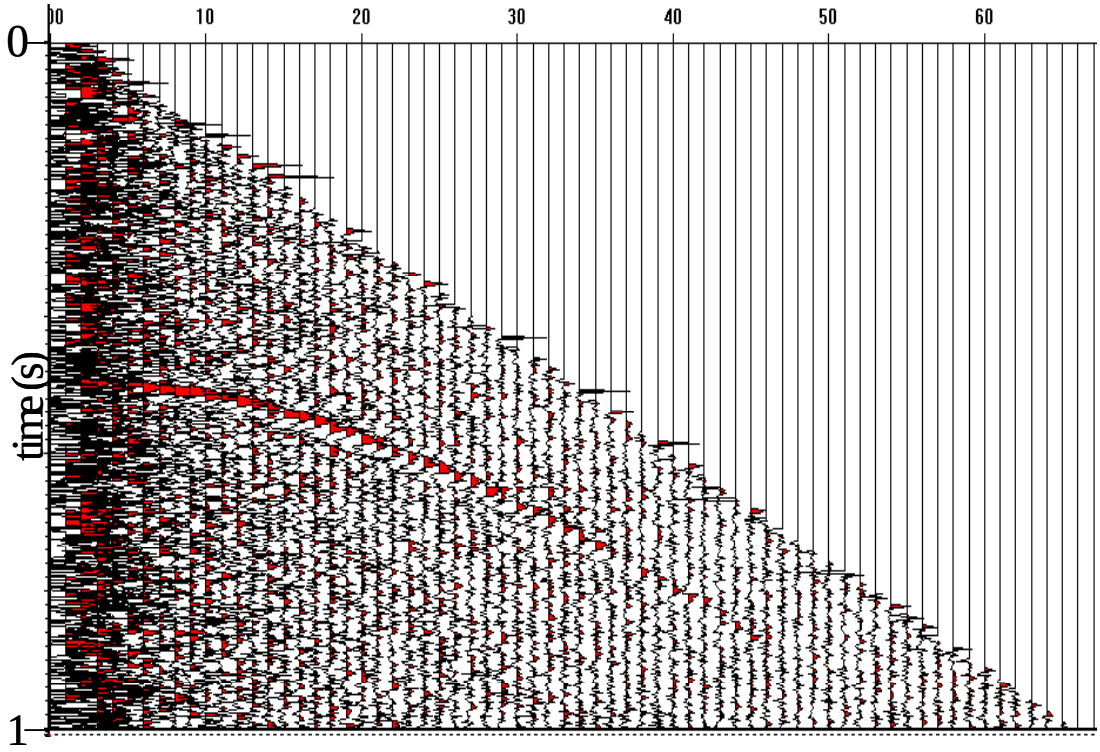

FIG.12. CSP gather located at x=1250m. No matched filter applied. Equivalent offset shown on x-axis, where dx=12.5m.

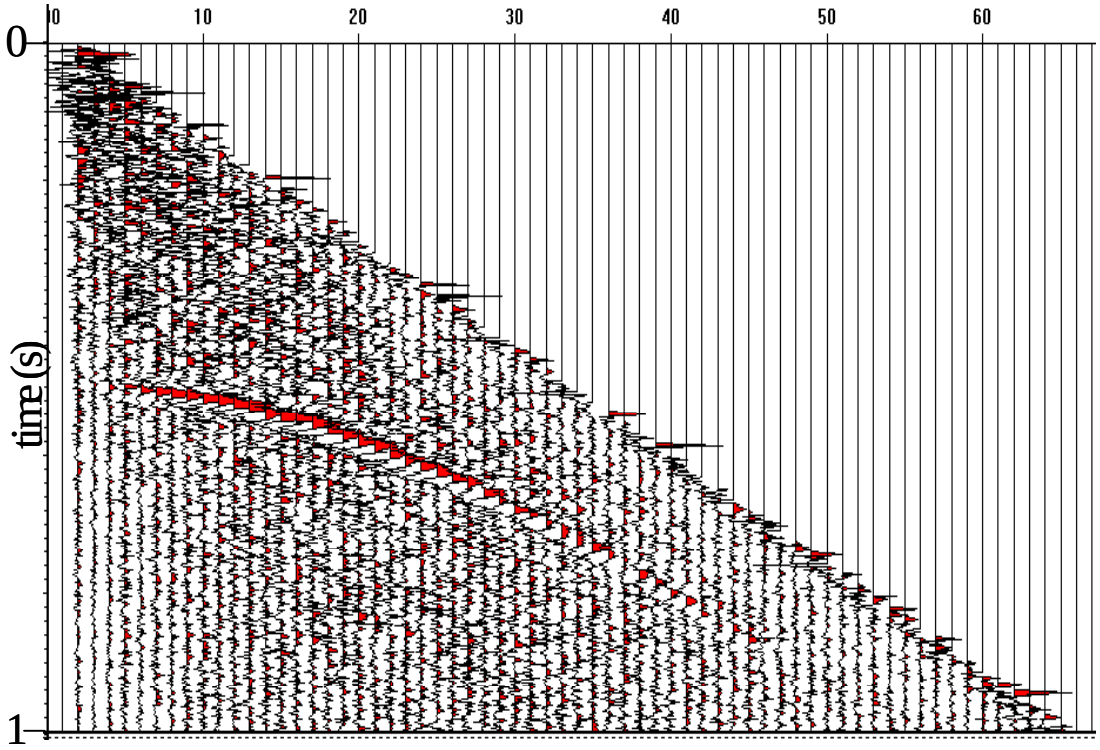

FIG 13. CSP gather located at x=1250m. Amplitudes scaled by the matched filter. Equivalent offset, shown on x-axis, where dx=12.5m.

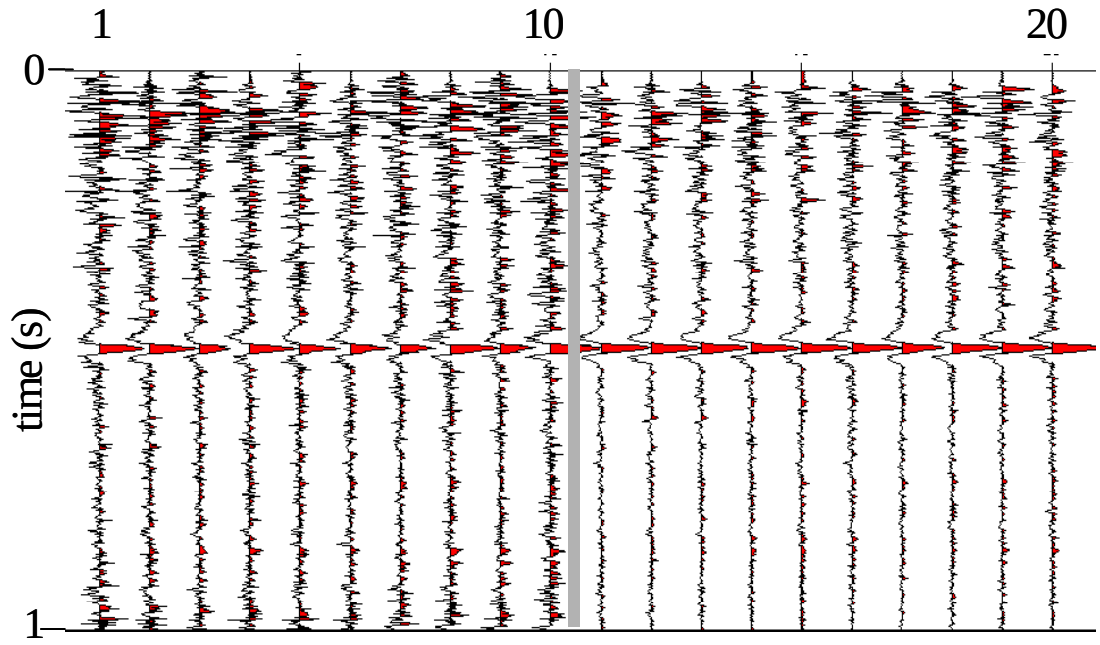

FIG.14. Traces 1-10 are migrated CSP gathers without matched filtering. Traces 11-20 are migrated CSP gathers located at the same positions, but have been match filtered.

SUMMARY

Preliminary analysis demonstrates the effectiveness of the matched filter in improving the S/N ratio in prestack migration given the simple synthetic example. Future work includes adding features to the migration algorithm such as a dip-limit taper, and a T_0/T scaling factor.

ACKNOWLEDGEMENTS

I would like to thank the following people for their assistance: Dr. John Bancroft, Kevin Hall, Henry Bland, and Marco Perez.

Thanks to the CREWES sponsors for their support.

REFERENCES

Bancroft, J.C., Geiger, H.D., and Margrave, G.F., 1998, The equivalent offset method of prestack time migration: Geophysics, **63**, 2042-2053

Bancroft, J.C., 2000, A practical understanding of pre- and poststack migrations, Course Notes Series, SEG publication

Lathi, B.P., 1965, Communication Systems, John Wiley & Sons

Robinson, E.A., Treitel,.S.,1980, Geophysical Signal Analysis, Prentice-Hall, Inc.

Wang, Shaowu, Bancroft, John C. and Lawton, Don C., 1996, Converted-wave (P-SV) prestack migration and migration velocity analysis, 66th Ann. Internat. Mtg: Soc. Of Expl. Geophys., 1575-1578.